Haukur Ingason, Fredric Seco

# Numerical simulation of a model scale tunnel fire test

## Brandforskprojekt 404-011

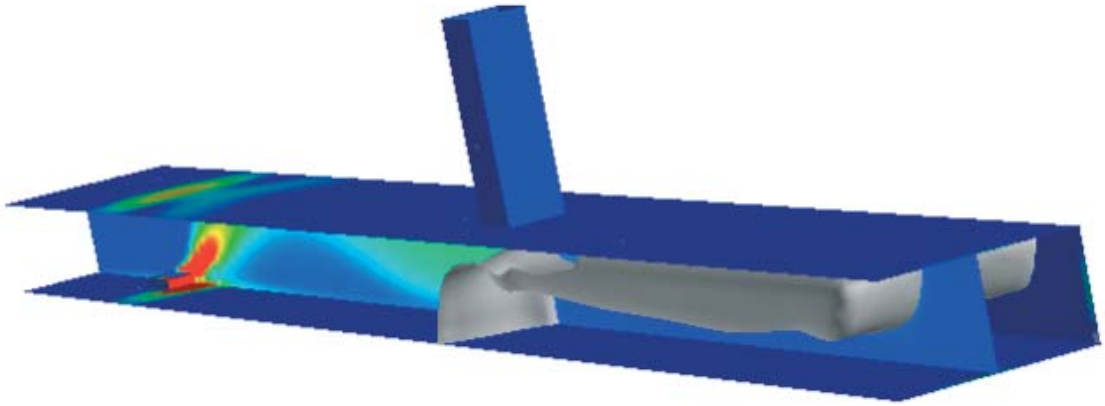

SP Fire Technology
SP REPORT 2005:47

SP Swedish National Testing and Research Institute

Haukur Ingason, Fredric Seco

# Numerical simulation of a model scale tunnel fire test

Brandforskprojekt 404-011

# Abstract

## Numerical simulations of a model scale tunnel fire test

Numerical simulations of a fire in a model scale tunnel with the CFD code FLUENT are presented. The objective of this study is to compare CFD simulation to experimental data obtained from a well defined model scale tunnel tests. A sensitivity analysis was carried out in order to find the best combination of physical models and grid structure for the type of application used here.

Key words: numerical simulations, CFD, extraction of smoke, model tunnel

**SP Sveriges Provnings- och Forskningsinstitut**
SP Rapport 2005:47
ISBN 91-85303-79-8
ISSN 0284-5172
Borås 2005

**SP Swedish National Testing and Research Institute**
SP Report 2005:47

Postal address:
Box 857,
SE-501 15 BORÅS, Sweden
Telephone: +46 33 16 50 00
Telex: 36252 Testing S
Telefax: +46 33 13 55 02
E-mail: info@sp.se

# Table of Content

# Förord

Denna studie ingår i Brandforsk projektet ”Inverkan av brandgasventilation på rök- och brandspridning i tunnlar och gruvor”. De CFD beräkningar som presenteras i rapporten genomfördes av en fransk student Fredric Seco från ENSIMEV – University of Valenciennes i Frankrike, som genomförde sin 5 månaders praktik vid SP våren 2002 under handledning av Haukur Ingason vid SP Brandteknik.

# Sammanfattning

Målsättningen med projektet är att undersöka möjligheterna att kombinera frånluftsventilation och längsventilation i tunnlar. För att optimera en sådan lösning krävs en parameterstudie där alla viktiga flödesparametrar undersöks. Det effektivaste sättet att göra en sådan parameterstudie är genom CFD beräkningar. Första steget är att göra en validering av det CFD program som ska användas för parameterstudien mot en applikation som liknar den som parameterstudien gäller. I vårt fall har vi valt att använda CFD koden FLUENT . Det är en väldokumenterad kod som har använts inom olika ingenjörsområden. Den har dock inte använts för den applikation som projektet avser.

En rad modellskaleförsök genomfördes på uppdrag av Brandforsk vid FOI (tidigare FOA) i samarbete med SP [1] där samverkan mellan frånluftsventilation och längsventilation undersöktes. Dessa försök är mycket väldefinierade och passar bra för validering av CFD koder. För validering av FLUENT valdes ut ett försök som ansågs vara representativt för den parameterstudie som genomfördes i den andra delen av projektet och som redovisas i en separat rapport [2].

Valideringen visar att resultaten överensstämmer kvalitativt bra med uppmätta data men kvantitativt överensstämmer det sämre. Simuleringarna visar att det finns många parametrar som kan inverka på resultaten. Många av de experimentella observationer som gjordes kunde förklaras med hjälp av simuleringarna, speciellt flödesbilden kring frånluftsöppningen. Det som tog mest tid var modelleringen av brandkällan och geometrin av denna. Det visade sig också att resultaten var känsliga för hur gridnäntet byggdes upp. Det var nödvändigt att göra en del lokala finfördelningar av gridnätet för att få programmet att konvergera.

Sammanfattningsvis så kan man konstatera att FLUENT ger rimliga resultat och att resultaten överensstämmer kvalitativt bra för denna typ av applikation. Därför har programmet använts med de inställningar som överensstämde best med de experimentella resultaten för den parameterstudie som beskrivs i [2].

Denna sida (6) skall vara blank!

# 1 Introduction

Ventilation system is one of the most important safety systems to be used in tunnel fires. It controls the spread of heat and smoke and is essential in order to create a safe environment for evacuation of people and when fighting fires in tunnels. The use of longitudinal ventilation in road tunnels has increased dramatically during the last decade. In recent years the combination of large opening extraction systems and longitudinal systems has been discussed. There is, however, limited experimental information available about the efficiency of these combined systems [3]. Ingason and Werling [1] have carried out well defined tests in a model scale tunnel which combine the longitudinal ventilation with a single point extraction opening.

It is well known that CFD (Computational Fluid Dynamics) programs are a very powerful tool when designing ventilation systems in tunnels. These programs need, however, to be validated for different types of applications. They do not give general solutions for all applications and scenarios. Therefore, they need to be “calibrated” for different situations. There are numerous physical models and constants that can be applied in these models but they are highly dependent on the type of application. A sensitivity analysis was carried out in order to find the best combination of physical models and grid structure for the type of application used here.

The aim of the study here was to investigate the possibilities and limitations when using the CFD code FLUENT [4], for simulation of single point extraction and longitudinal ventilation. By using a simple and well defined experimental case it is possible to understand the main phenomena, and thereby establish the efficiency or weakness of the combined system. It is of special interest to investigate the risks and thresholds for continuous smoke spread along the tunnel when using a combined system of extraction and longitudinal flow. The next step in the study is presented in a separate report [2]. This includes a parametric study of the influence of the size of opening and ventilation rate on the efficiency of such a system.

# 2 Experimental Set-up

Smoke spread tests have been performed in a model tunnel measuring 2 m wide, 1 m high and 20 m long [1]. The material on the walls, floor and ceiling consisted of 12 mm Promatec fibre-silica board, except for one side-wall which consisted of 5 mm thick fire resistant window glass. The window was used to visually document the smoke spread. The floor boards were elevated 0,1 m from the concrete floor by a wooden frame system. The fire load consisted of a Kerosene pool fire located 2.5 m from one end of the tunnel. Two different pan sizes were used, 0.33 x 0.33 m and 0.4 x 0.4 m, respectively. The exhaust ventilation arrangement and the longitudinal velocity were varied. Different numbers of thermal shafts were mounted along the tunnel at locations A, B and C. Mechanical ventilation was arranged in shaft B in Figure 1.

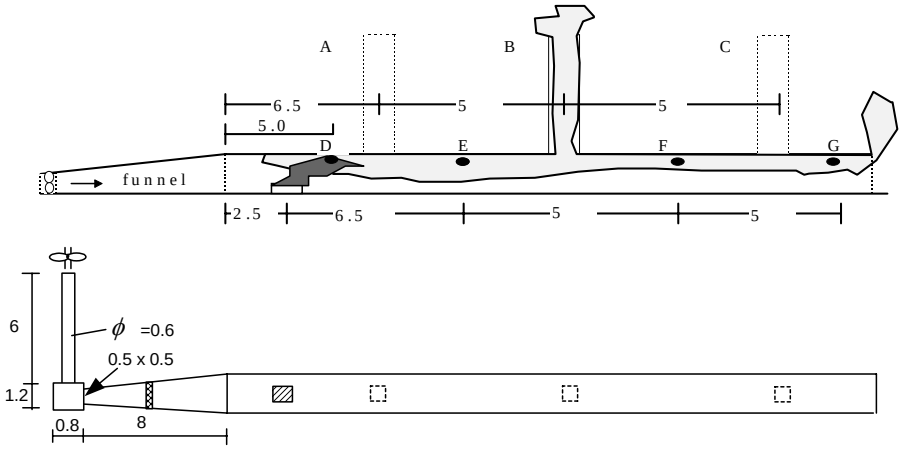


Figure 1 The experimental set-up. All dimensions are in meter. The upper drawing is a side view, the lower drawing is a plan view.

A specially designed funnel shaped tunnel was attached to one end of the tunnel in order to create a uniform flow over the cross-section at the tunnel entrance, see Figure 1. The other end of the tunnel was fully open. Extensive effort was put into creating a uniform air flow over the tunnel cross-section prior to ignition of the fire. The fan was attached to a 6 m long circular tube with diameter of 0,6 m, which in turn was connected to a closed wooden box which measured 1.2 m by 0,8 m and 1,4 m high. The funnel was then connected (at a 90 degree angle in relation to the tube) with this box through a 0,5 m x 0,5 m opening at floor level. An aluminium alloy flow-straightener in a honeycomb pattern was placed about 4 m from the box. Thus, the swirl velocity created by the fan was evened out in the box and the 8 m long funnel. The flow at the entrance of the tunnel became very uniform and stable.

Measurements were performed at four different locations downstream of the fire: i.e., locations D, E, F and G, see Figure 1. The measuring points were placed along the centreline of the tunnel. The optical density was measured at E, F and G with optical density meters (photocell and lens) over the path length of 2 m. The optical density was converted to smoke concentration by divide the measured value with the smoke extinction coefficient 3300 $m^2/kg$. The oxygen concentration was measured at E, F and G, 0.25 m below ceiling, along the centreline of the tunnel. Oxygen concentrations ($O_2$) were measured by sucking the gases through a probe consisting of a copper tube (Ø 6 mm) connected to an analyser. The thermocouples were of type K with a wire diameter of

0.25 mm, chromel-alumel, 1200 °C range and mounted at each station (D, E, F and G) at heights 0.1, 0.3, 0.5, 0.7, 0.8 and 0.9 m above the floor. The velocity was measured using bi-directional probes. They were placed 0.9 m above floor at locations D, E, F and G and at 0.5 m above floor at locations E and F.

In order to measure the mass burning rate the Kerosene fuel pan was placed on a weighing platform located under the floor of the tunnel (see Figure 2). The floor consisted of 12 mm Promatec silica board. The distance between the Promatec floor and the concrete floor of the test hall was 95 mm. Four 30 mm high stainless steel rods were put through the Promatec floor. Any friction to the Promatec boards was prevented by drilling the holes slightly wider than the rods. No influence of heating on the results was observed. The gas temperature close to the load cell did not increase more than 2 °C during the test. The accuracy of the load cell was +/- 1 g.

Figure 2 A photo of the model scale test tunnel. The fire source consisted of a Kerosine fuel.

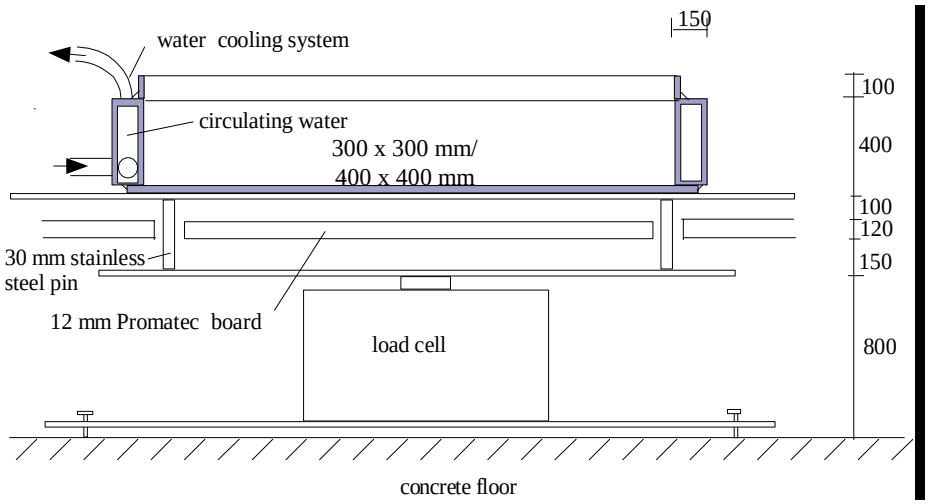


Figure 3 A cross-sectional view of the weighing platform and the fuel pan.

Table 1 The experimental program using thermal shafts.

| Test no | Air velocity (m/s) | Shaft (height/width/ length) (m/m/m) | Number of shafts | Fire source (m x m) | Average $m_f$ (g/s) | Q (kW) |
|---|---|---|---|---|---|---|
| 01 | 0 | 1/0.4/0.4 | 3 | 0.33 x 0.33 | 0.97 | 38.3 |
| 02 | 1 | --- ” --- | --- ” --- | --- ” --- | 1.07 | 42.3 |
| 03 | 0 | 3/0.4/0.4 | --- ” --- | --- ” --- | 0.83 | 32.7 |
| 04 | 0.5 | --- ” --- | --- ” --- | --- ” --- | 0.78 | 30.9 |
| 05 | 0.75 | --- ” --- | --- ” --- | --- ” --- | 0.76 | 29.9 |
| 06 | 1 | --- ” --- | --- ” --- | --- ” --- | 1.04 | 40.9 |
| 07 | 0 | --- ” --- | --- ” --- | 0.4 x 0.4 | 1.35 | 53.4 |
| 08 | 1 | --- ” --- | --- ” --- | --- ” --- | 1.39 | 54.9 |
| 09 | 0.75 | --- ” --- | --- ” --- | --- ” --- | 1.27 | 50.3 |
| 10 | 0.5 | --- ” --- | --- ” --- | --- ” --- | 1.18 | 46.6 |
| 11 | 0.5 | 3/0.4/0.4 | 1 | --- ” --- | 1.23 | 48.7 |
| 12 | 0.75 | --- ” --- | --- ” --- | --- ” --- | 1.24 | 49.0 |
| 13 | 1 | --- ” --- | --- ” --- | --- ” --- | 1.49 | 59.0 |
| 14 | 0 | --- ” --- | --- ” --- | --- ” --- | 1.82 | 71.9 |
| 15 | 0.5 | 3/0.2/0.2 | --- ” --- | --- ” --- | 1.22 | 48.3 |
| 16 | 1 | --- ” --- | --- ” --- | --- ” --- | 1.77 | 70.0 |
| 17 | 0 | closed | 0 | --- ” --- | 2.01 | 79.4 |
| 18 | 1 | --- ” --- | --- ” --- | --- ” --- | 1.45 | 57.4 |
| 19 | 0.75 | --- ” --- | --- ” --- | --- ” --- | 1.25 | 49.2 |
| 20 | 0.5 | --- ” --- | --- ” --- | --- ” --- | 1.31 | 51.8 |
| 21 | 0 | --- ” --- | --- ” --- | 0.33 x 0.33 | 0.86 | 33.9 |
| 22 | 1 | --- ” --- | --- ” --- | --- ” --- | 1.04 | 41.0 |
| 23 | 0.75 | --- ” --- | --- ” --- | --- ” --- | 0.76 | 29.9 |
| 24 | 0.5 | --- ” --- | --- ” --- | --- ” --- | 0.77 | 30.3 |
| 25 | 0.5 | 3/0.6/0.6 | --- ” --- | 0.4 x 0.4 | 1.30 | 51.3 |
| 26 | 1 | --- ” --- | --- ” --- | --- ” --- | 1.41 | 55.9 |

Table 2 The experimental program for mechanical ventilation.

| Test no | Air velocity (m/s) | Shaft (height/width/ length) (m/m/m) | Exhaust ventilation ($m^3/s$) | Fire source (m x m) | Average $m_f$ (g/s) | Q (kW) |
|---|---|---|---|---|---|---|
| 27 | 0 | 2/0.6/0.6 | 2 | 0.4 x 0.4 | 1.56 | 61.62 |
| 28 | 0 | --- ” --- | 2.7 | --- ” --- | 1.14 | 45.03 |
| 29 | 1 | --- ” --- | 2.7 | --- ” --- | 1.51 | 59.64 |
| 30 | 1 | --- ” --- | 1.56 | --- ” --- | 1.43 | 56.49 |
| 31 | 1 | --- ” --- | 2 | --- ” --- | 1.42 | 56.09 |
| 32 | 1 | --- ” --- | 2.3 | --- ” --- | 1.63 | 64.39 |
| 33 | 0.5 | --- ” --- | 2 | --- ” --- | 1.35 | 53.33 |
| 34 | 1 | --- ” --- | 2.7 | --- ” --- | 1.50 | 59.25 |
| 35 | 2 | --- ” --- | 2 | --- ” --- | 1.89 | 74.26 |
| 36 | 2 | --- ” --- | 2.7 | --- ” --- | 1.87 | 73.87 |

Extensive work was carried out to obtain a steady mass burning rate during the pool fire tests with Kerosene. Usually the rim of a fuel pan will be warmed up and the heat balance at the fuel surface will continuously change. This will result in a mass burning rate which is unsteady during the fire test. For the small fuel pans used here this can be a great problem. The simplest way to obtain steady state conditions is by controlling the heat balance. This can be done by cooling the rim by circulate water. The problem is to find the appropriate geometry of the rim and an appropriate water flow rate.

After extensive work it was found that, for the square pans used, the best results were obtained with a water flow rate of 2 litre/minute and a cross sectional area of the rim of 15 mm wide and 50 mm high. The rim itself consisted of a square steel measuring 15 mm x 40 mm with either a 300 x 300 mm steel sheet or 400 x 400 mm (the bottom of the fuel pan) welded to the U-profiles. In order to avoid fuel leaking over the edge of the rim a 10 mm high steel edge was welded on the top of the rim. Thus, the height of the inner surface of the pan was 50 mm. The water cooled part was 40 mm. The thickness of the steel used in the rim was 2 mm. The temperature of the water flowing into the rim of the fuel pan was 10 °C and the water temperature flowing out from the rim was about 30 - 35 °C. In Figure 4, typical mass burning rate curves are shown for two different pan sizes. This method is found to be very robust and cheap. The mass burning rate became stationary after only 1-2 minutes.

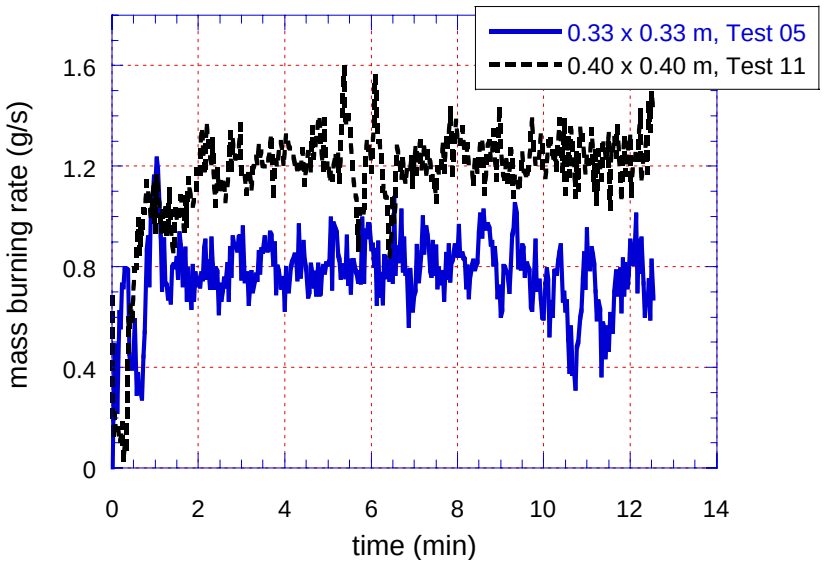


Figure 4 Mass burning rate of Kerosene measured with water cooled rims. Result using two different pan sizes are shown, 0.33 x 0.33 m and 0.40 x 0.40 m, respectively.

Every test was run for 12 minutes in order to obtain stationary conditions within the tunnel. It is difficult to obtain stationary wall temperatures but the gas temperatures were found to be quite stationary. In Figure 5, a plot is given of the gas temperature and the ceiling temperature at location E. The ceiling temperature was measured by drilling an 11 mm deep hole in the Promatec board from the top. Thus 1 mm remained to the exposed surface at station E. The thermocouple was glued into the hole to obtain a good contact with the material. As can be observed in Figure 4, the gas temperature (0.1 m from ceiling at E) is quite stationary whereas the ceiling is still warming up at the end of the test.

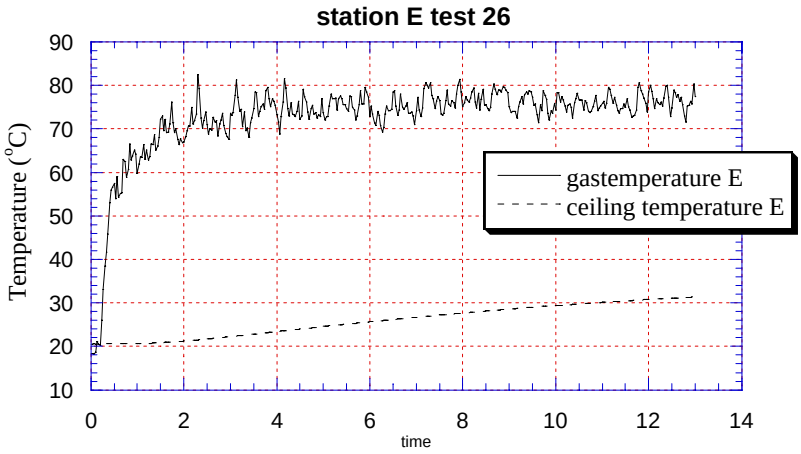


Figure 5 Gas temperature 0.9 m above floor and ceiling temperature 1 mm from the exposed ceiling surface at station E.

# 3 Simulation of the model scale tunnel

## 3.1 Geometrical representation of the model scale tunnel

The model scale tunnel was simulated with the CFD program FLUENT [4]. In Figure 6, a geometrical representation of the model tunnel is shown. This figure shows the grid size used and the central plane along the tunnel where the temperature contours are plotted in different colours. Simulations were performed for a case with a single point smoke extraction system and with a longitudinal flow along the tunnel. The location of the kerosene tray is indicated by the red colour. Due to the longitudinal ventilation, the flame is tilted. This flame tilt can be observed both in Figure 6 and in Figure 2.

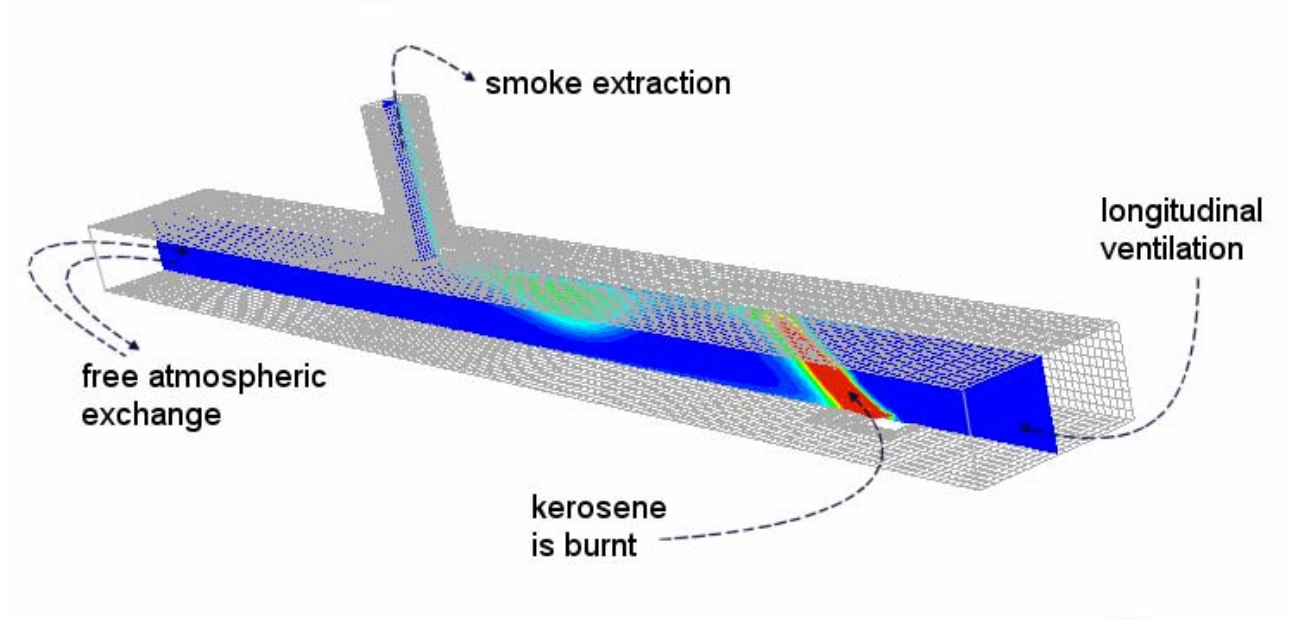


Figure 6 A geometrical representation of the test tunnel as applied in FLUENT.

In Figure 7, the geometrical dimensions of the model as used in the simulations, are shown. The width and the depth of the shaft are 0,6 m x 0,6 m, respectively, and the height is 2 m. The tunnel itself was 2 m wide and 1 m high and the distance from the fuel source to the shaft was 9 m. As described in chapter 2, a 6 m long tube and 8 m long funnel was attached to the entrance of the tunnel (upstream side, see Figure 1). This was done to avoid swirl velocities caused by the ventilation fan. This part of the tunnel, the tube and the funnel, were not modelled here but it was assumed that the flow was fully developed and uniform when it entered the tunnel entrance 2.5 m upstream of the fire source. This simplification is reasonable since uniform flow was confirmed at the entrance of the tunnel.

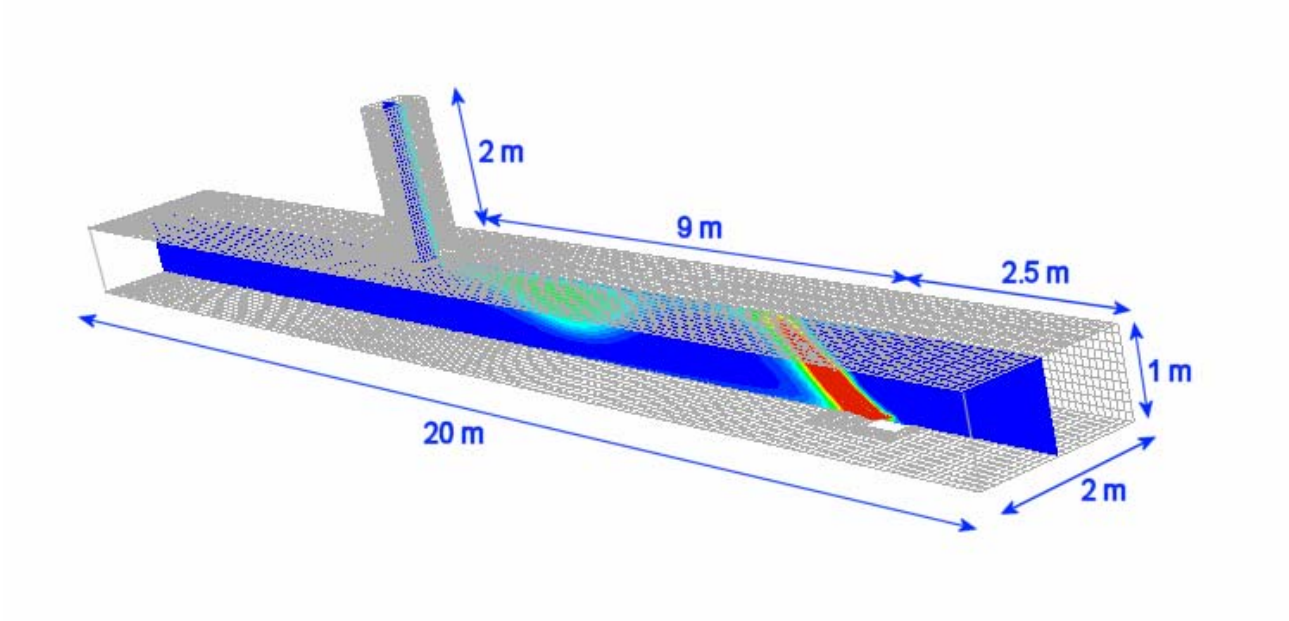


Figure 7 The geometry of the model tunnel as it was applied in the simulations.

In Figure 8, a simple sketch of the kerosene fuel pan is given, which was positioned on the floor. Different types of modelling of the fuel source were tested. This is explained in more detail in section 5.1.4.

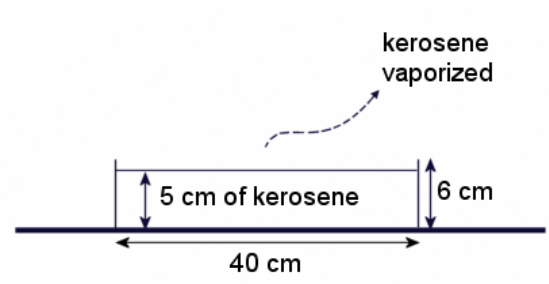


Figure 8 Simple sketch of the kerosene fuel pan.

All other details on the mass burning rate measurements and other instrumentation are given in chapter 2. In Table 3, the location of the instrument stations along the tunnel are given. The identification of each instrument station can be obtained in Figure 1.

Table 3 Locations of the measuring stations according to Figure 1.

| Measuring station | Location |
|---|---|
| D | 5 m far from the entrance |
| E | 9 m far from the entrance |
| F | 14 m far from the entrance |
| G | 19 m far from the entrance |
| Ceiling-line | Line along the tunnel 10 cm below the ceiling |

## 3.2 The reference case

As shown in Tables 1 and 2, a total of 36 tests were performed. One reference test, which was deemed to be representative of the situation of interest here, namely test 29, was chosen. In this test, the longitudinal ventilation was 1 m/s, the mass flow rate of liquid

kerosene applied in the tunnel was 1,51 g/s and the mechanical extraction of 2,7 $m^3/s$ was provided through the shaft which was 2 m high, 0.6 m wide and 0.6 m deep, see Figure 9.

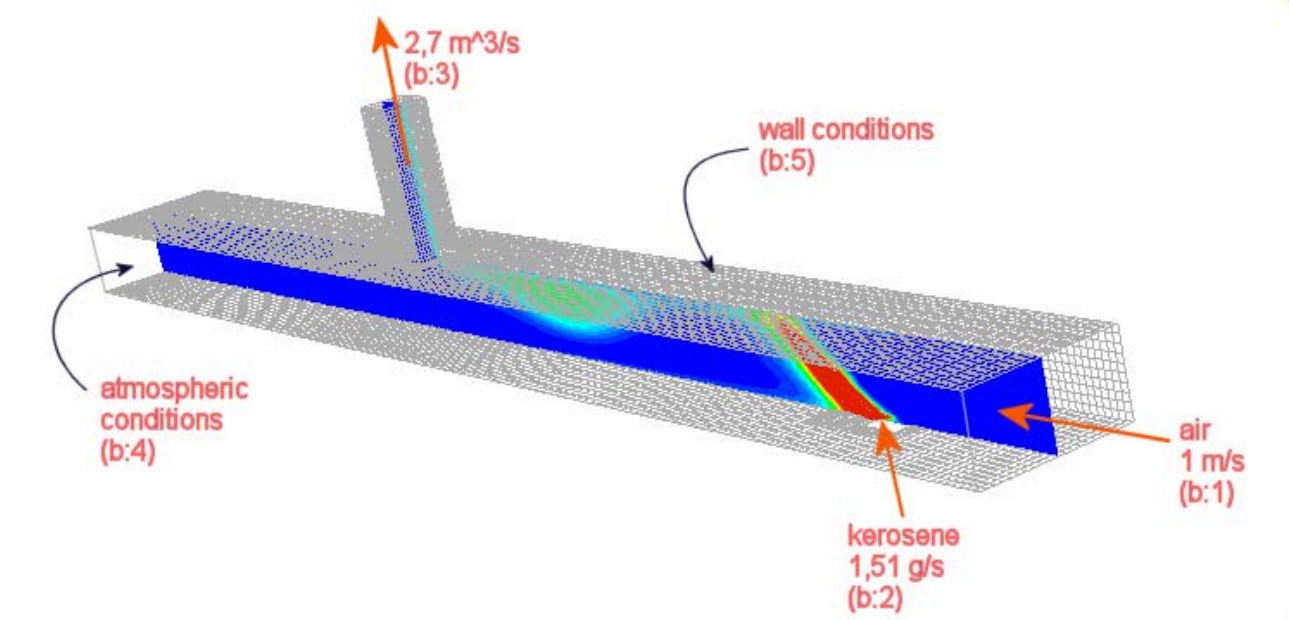


Figure 9 Conditions of the reference case (test 29 in Table 2).

## 3.3 Modelling the reference case with FLUENT

### 3.3.1 Generation of the geometry

Different geometries were established with the GAMBIT pre-processing program for FLUENT. The geometry of the experimental set-up was modelled as accurately as possible. Changes in the geometry were only made for the fuel-inlet. Many numerical tests were performed to model the fuel pan. It was found that the simulations were very sensitive to geometrical changes as can be seen in section 5.1.4.

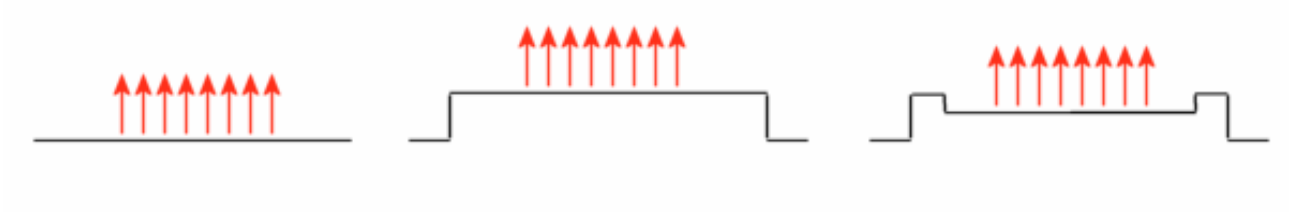

Figure 10 Different numerical models for the fuel pan which were tested.

### 3.3.2 Boundary conditions

The boundary conditions were slightly simplified compared to the experimental set-up. For example, the fan was replaced by a velocity-inlet, without any consideration to the funnel shaped tunnel in front of the entrance. There were 5 different boundary conditions that were prescribed for the reference case (see Figure 9):

- the longitudinal ventilation (b:1),
- the fuel inlet (b:2),
- the shaft extraction (b:3),

- atmospheric conditions (b:4),
- two diffferent walls (b:5): one made of 5 mm glass and the other of 12 mm Promatect H boards (see Figure 2).

More detailed information about each of the boundary conditions is given below.

Longitudinal ventilation (b:1):
A velocity inlet was used with a pre-set velocity of 1 m/s at the entrance. In the experimental case, this flow was provided by a fan located 15 m from the inlet (see Figure 1). The flow swirls that were created in the funnel, were adjusted with the aid of Honeycomb flow straightener placed in the funnel, 4 m from the entrance.

The fuel-inlet (b:2):
Mass flow inlet with 1,51g/s of kerosene vapour. The mass fraction was set to 1 for kerosene and the temperature was set to 70°C (kerosene vaporization at 70°C). During the course of this work it was found that it was not easy to use a velocity-inlet type of condition for the fuel, i.e., it was much better to work with a mass flow rate-inlet type.

The shaft (b:3):
Velocity inlet was used here since it was better to define a specified velocity at the boundary instead of a mass flow rate. FLUENT uses wall functions for calculating velocities close to the walls. Due to this, an error in the mass flow rate will occur when setting a constant velocity on the top surface of the shaft. Therefore, we had to adjust the extraction velocity in order to obtain the right mass flow rate. The mass flow rate was set to 3 kg/s, which corresponds to 2,5 $m^3/s$ (instead of 2,7 $m^3/s$ as in Table 2) and a outlet velocity of 6,95 m/s (cross-section of the shaft is 0,36 $m^2$).

The exit (b:4):
Pressure outlet with the possibility of a backflow was used. Note that there is no gauge pressure, i.e., the pressure outlet is similar to a free atmospheric surface at the entrance. The ambient temperature was set to 13 ºC.

The wall (b:5):
As in the experiments two different solid materials were used: glass and Promatect H boards. One side of the model tunnel consisted of a 5 mm thick glass and the rest was made of 12 mm thick Promatect H boards. For heat transfer through the walls, convection and radiation for the internal faces, conduction in the wall, and convection for the external faces were considered. The sensitivity of different solutions to these boundary conditions was also examined.

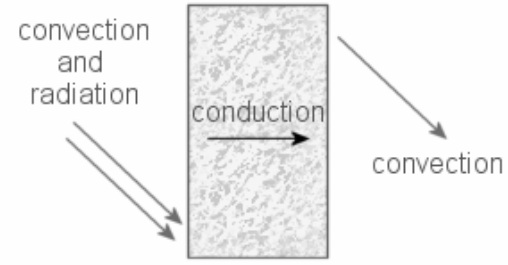


Figure 11 Heat transfer at the wall boundary.

### 3.3.3 Grid generation

It was found most suitable to use hexahedral cells rather than tetrahedral cells. The grid was made finer in the fire area and near the shaft. The main reason for these refinements was to obtain more accurate results while minimising computer time. In Figure 12 the refined grid is shown for the fire source and the single point extraction shaft.

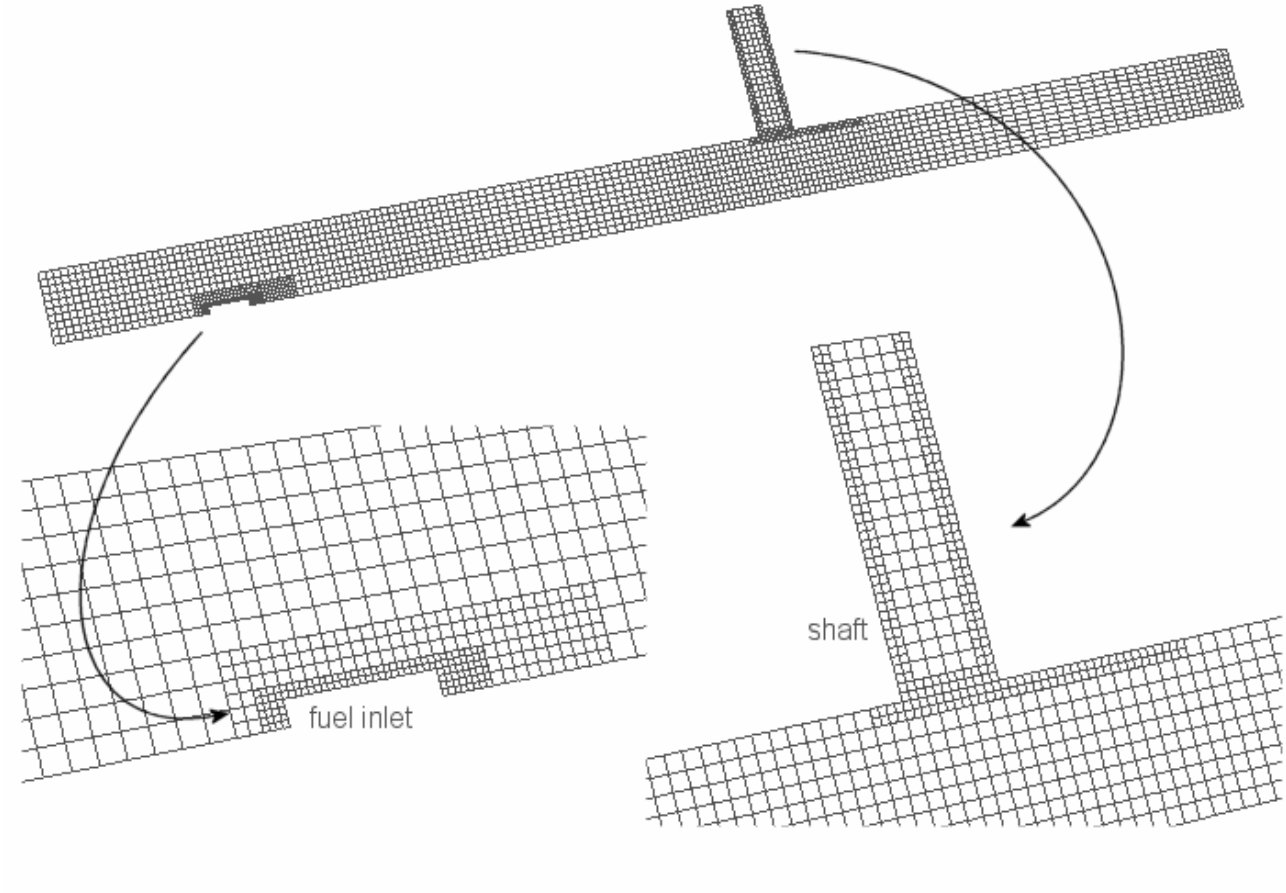


Figure 12 Example of grid structure at the middle section of the tunnel. The refinements at the fire location and at the shaft are shown specifically.

The number of cells varied from 30 000 to 60 000. This corresponds to meshes of 10 cm, where the mesh was 5 cm with one refinement and 2,5 cm with two refinements (close to the fuel inlet).

### 3.3.4 Physical models

For the type of problem simulated here there are numerous physical models in FLUENT that need to be considered. Each of the models is discussed below together with which consequences the model choice may have on the results.

Turbulence models:
There are different turbulence models available in FLUENT. The model scale tunnel scenario is a combustion problem which means that the smallest turbulence model which is allowed is the K-ε model with full buoyancy effects. Unfortunately, this model does not work very well with low Reynolds numbers (as is the case here). Despite its

limitations it is the only realistic choice in this application due to the long computation time associated with any alternative turbulence model.

Mixture material:
The mixture of air–kerosene(v) is prescribed in FLUENT. Consequently, current parameters were defined by default. Different fluids were activated: kerosene(v), oxygen, carbon dioxide and water(v). All of these fluids were regarded as ideal gases and the properties of the mixture were regarded as a mix of the properties of the different fluids. For each fluid, the specific heat is dependent of the temperature and thermal conductivities. Viscosities were computed by kinetic theory.

Combustion models:
There are numerous combustion models available in FLUENT. In this study the simplest one was chosen: reaction without carbon monoxide, $NO_x$ and soot. Eddy dissipation was used for calculating the rate of the reaction (the Arrhenius limits were also tested):

$$C_{12}H_{23} + 17{,}75 \cdot O_2 \Rightarrow 11{,}5 \cdot H_2O + 12 \cdot CO_2$$

Radiation models :
There are four different models of radiation available in FLUENT: Rosseland, P1, DTRM and DO. Three out of four models were tested. It was not possible to evaluate the DTRM model because it is not available with a refined grid.

### 3.3.5 Initialization and controls

In order to ignite the fire, a normal procedure in FLUENT is to assume high initial temperature. With regard to the discretization schemes the following options were chosen:

- *standard* for pressure,
- *simple* for velocity-pressure coupling,
- *1st order upwind* for momentum,
- *turbulence* and *species*,
- *2nd order upwind* for energy.

Under-relaxation factors were changed during the calculation to improve the solution's convergence.

# 4 Results

Different numerical models were tested and a comparative analysis was carried out in order to find the best converged solution. The objective was to comply as much as possible with the experimental test set-up. Once this process had been finalized it was possible to present some of the results and compare it to the experimental data.

## 4.1 Experimental results

The glazed window on the side of the tunnel in the experimental study facilitated documentation of the smoke spread in the tunnel. In Figure 13, the documented smoke spread from test 29 (reference test), is shown. Upstream of the fire source there was limited (1 – 1,5 m) backlayering of smoke. Between the fire source and the exhaust opening, an area with dense smoke (hot layer) close to the ceiling was observed. It was approximately 0,3 m thick. Below the thick smoke layer there was an intermediate smoke layer (mixing layer), approximately 0,3 – 0,6 m thick. Downstream from the exhaust opening there was a 5,5 m long backlayering of smoke (about 0,25 – 0,3 m thick).

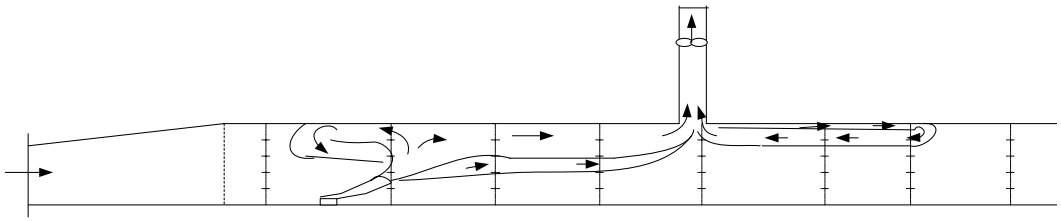

Figure 13 Smoke spread within the tunnel during test 29. The smoke backlayering distance is 5,5 m from the exhaust opening. Note the reversed flow to the right of the extraction opening.

Since the longitudinal ventilation rate was 2 $m^3/s$ (1 m/s x 2 $m^2$) upstream the fire and the extraction rate was 2,7 $m^3/s$, some air was sucked from the exit of the tunnel towards the extraction opening. However, this reversed velocity is not high enough to prevent backlayering downstream the extraction opening (see Figure 13) and therefore smoke was bypassing the extraction opening (0,6 m x 0,6 m) up to 5,5 m.

The measured average temperatures (average over the test period) along the ceiling have been used to compare the numerical simulations. In Figure 14, a plot is shown of the temperature for test 29, 0,1 m below the ceiling and in Figure 15 the vertical temperature distribution is shown at measurement stations D, E, F and G.

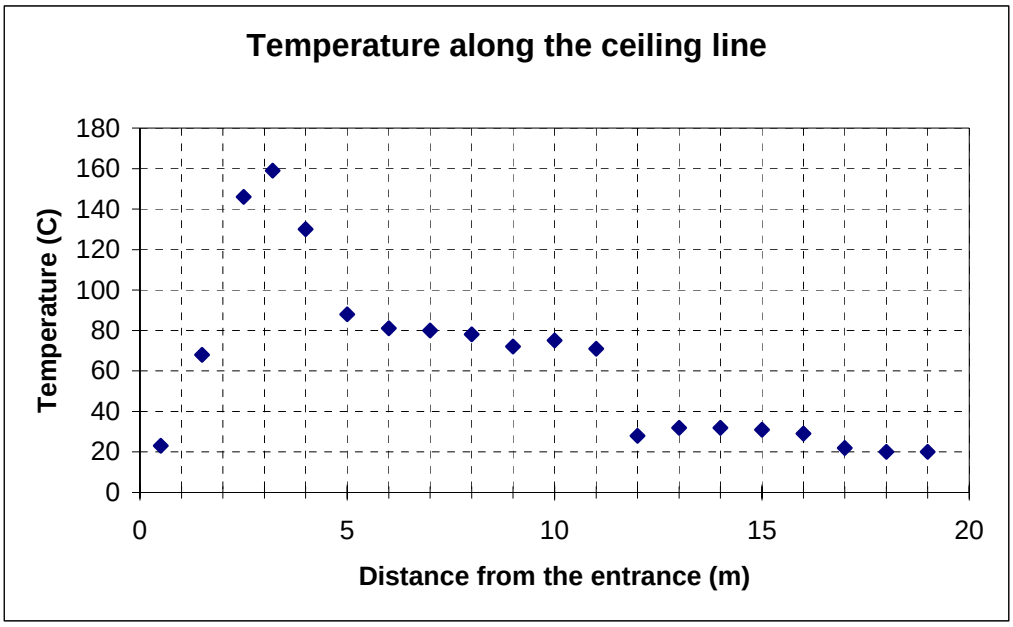


Figure 14 Measured centreline temperature (average over the test period) 0,1 m under the ceiling.

In Figure 14, we can observe both the peak temperature of 160 ºC and the location of the single point extraction shaft (strong temperature decrease between 11 – 12 m). The peak temperature is slightly offset from the centre of the fire. This is due to the longitudinal ventilation, which tilts the flame tip in the direction of the flow. The temperature between the fire and the shaft decreases relatively slowly.

## 4.2 Numerical calculations

To solve the reference case with no fire (called the “cold” solution here) 150 iterations at least were needed. When a fire is present in the model the calculation time increases considerably. Generally, it took between 300 and 1000 iterations to converge, which corresponds to between 1 and 3 hours. The quality of the initialization influences the convergence considerably. In most cases, it was better to use a closed solution that was already converged as an initialization for a new calculation.

Criteria of convergence are defined by default in FLUENT. Criteria for the numerical residuals of energy and radiation could be changed from $10^{-6}$ to $5 \times 10^{-6}$ without any consequences on the quality of the results. By doing this it was possible to speed up the computation time.

When the residuals did not change further, relaxation factors were changed. The momentum factor did influence the convergence speed considerably. In Table 4, the variations of main relaxation factors during the simulations are presented.

Table 4 The relaxation parameters used in the simulations.

| **Relaxation** | **High value (the beginning)** | **Low value (the end)** |
|---|---|---|
| pressure | 0,3 | 0,1 |
| momentum | 0,7 | 0,3 |
| energy | 1 | 0,7 |
| turbulence | 0,8 | 0,3 |
| viscosity | 1 | 1 |
| radiation | 1 | 0,7 |
| species | 1 | 0,1 |
| density | 1 | 0,7 |
| body forces | 1 | 1 |

## 4.3 Comparisons between numerical and measured temperature

In the following, a presentation of the optimized solution, is given. The calculation procedure is presented in more details below. Discussion and motivation are given for all the major problems that were solved during the course of this work.

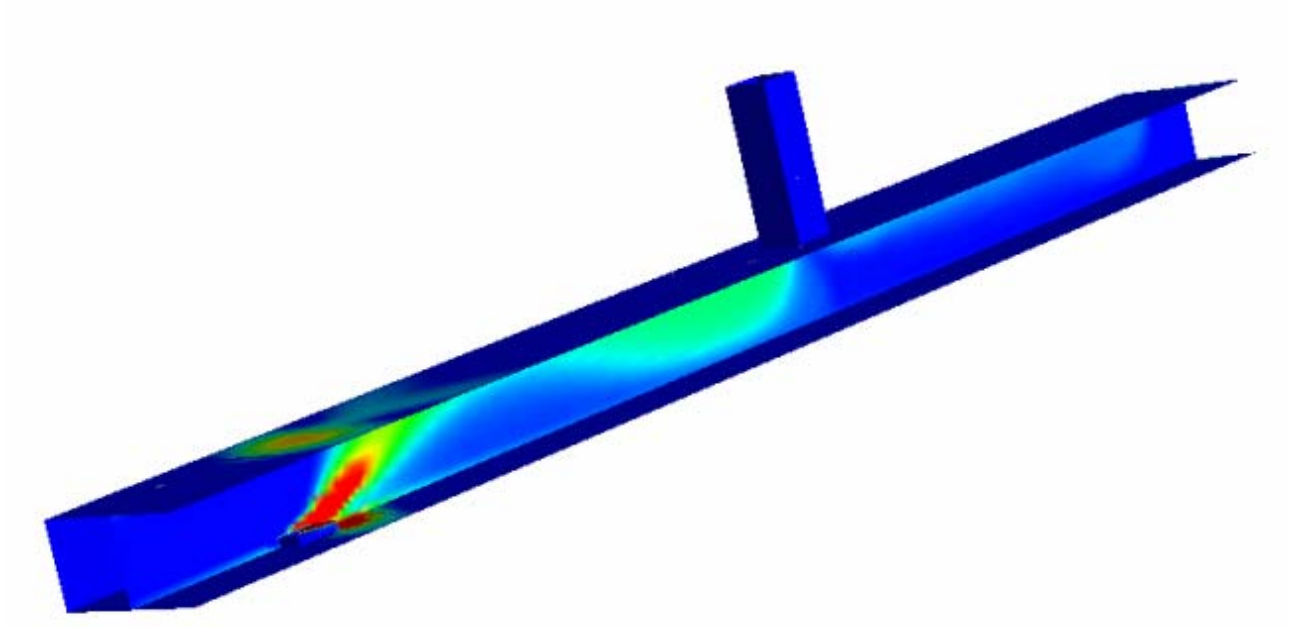

Figure 15 Temperature calculated in the model tunnel.

In Figure 15, the temperature at the centreline of the tunnel together with the temperature of the ceiling wall is shown. As can be seen in Figure 15, the temperatures are not homogenous downstream of the fire. The temperature is strongly dependent on the distance from the fire, which was also observed in the experiments.

Further, close to the top of the fuel-inlet, the wall temperature is very high because of radiation from the fire. The simulations show that there will be backlayering behind the

shaft, as was seen in the experimental case. The length of this backlayering was estimated to be 7,5 m (experimentally this was measured to 5,5 m).

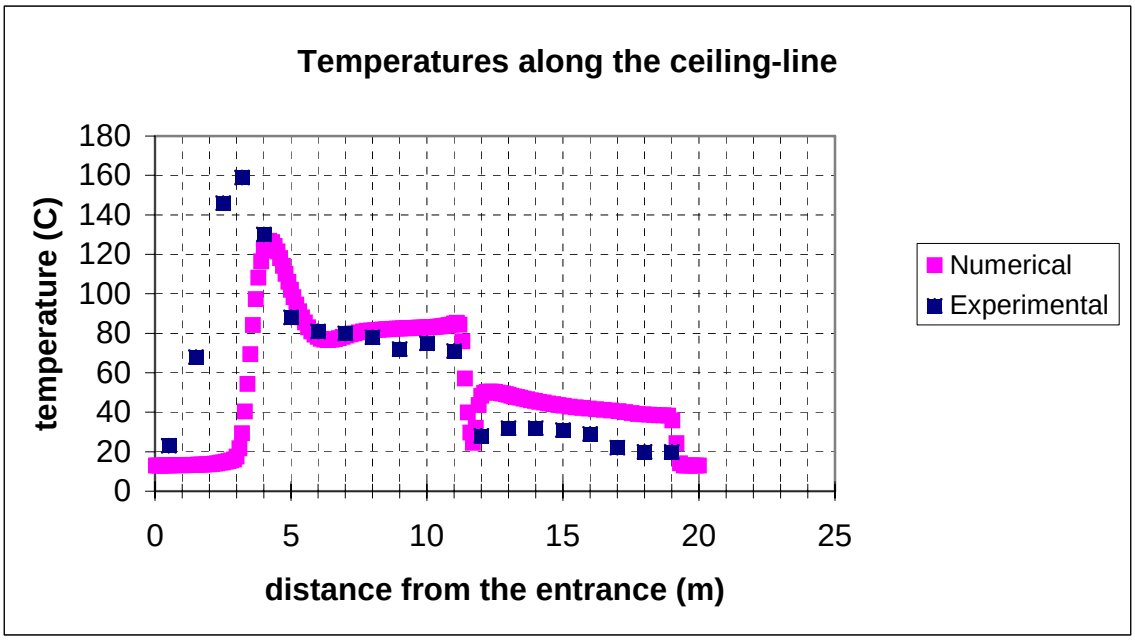


Figure 16 Numerical and experimental temperature values along the ceiling.

Figure 16 shows a comparison between the experimental and calculated data. The curves are quite similar in shape but there are some differences in the results close to the fire. The temperature peak differs by 30°C and the backlayering temperatures differ by 20°C. The radiation calculations give 2,4 kw/m$^2$ at station E (0,9 m above the floor), compared to 0,9 kw/m$^2$ experimentally. The numerical values of the velocity were found to be quite similar to the experimentally obtained values.

The numerical and experimental results are qualitatively similar but there are some local differences in the results. This indicates the main problem with comparison of experimental and calculated data. There are always some differences due to the many factors that can influence the results. It is impossible to obtain exactly the same results but it is very important that the results are qualitatively equivalent.

In the following we will point out and discuss in more detail some problems that we have experienced during the course of this work.

# 5 Discussion

## 5.1 Problems and choices

### 5.1.1 Grid improvements

The result verifies that it was not necessary to model the funnel in front of the tunnel entrance. As discussed previously, the funnel was connected to the tunnel to minimize the swirl velocities at the entrance of the tunnel.

In order to reduce the calculation time, an attempt was made to simulate half of the tunnel by splitting it up along the centre line (symmetry line). In the experiments the tunnel was not fully symmetrical because one side of the tunnel was mounted with a glazed window. Thus, the symmetry calculations did not work properly. There were some unexplainable results obtained. The wall temperature became too high and finally it was decided to simulate the tunnel with Promatect H boards on one the wall, the floor and the ceiling and the glazed window on one side. The results became much more stable and thereby more reasonable.

An important lesson learned is that the quality of the solution not only depends on the convergence and the residual values. The quality of the grid was also found to be very important. For example, if some minor changes were made to the geometry, it was necessary to add smaller meshes surrounding the changes otherwise the changes were ignored by the program.

### 5.1.2 Radiation's model

Among the different radiation models, one model was found to be inadequate for the application simulated here. Figure 17 below, shows the difference between results with the Rosseland model and a DO model (the reference case is simplified here; there is no extraction in the tunnel).

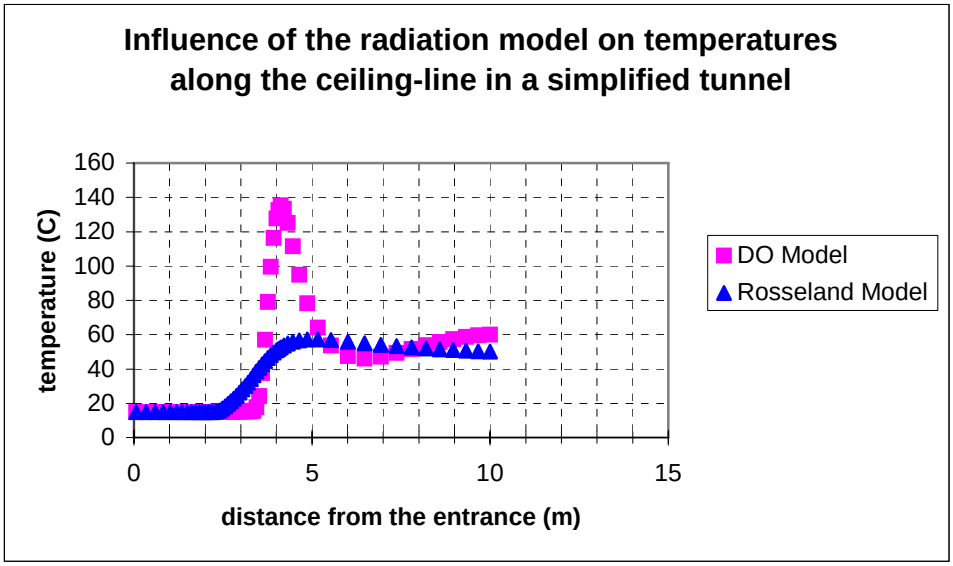


Figure 17 Rosseland model was found to be inadequate for the application simulated here (Note: no extraction simulated in the tunnel).

The Rosseland model is not acceptable to use in this kind of problem. The DO model and the P1 model appears to be good enough. The DO model was selected because according to FLUENT ’s documentation, P1 could tend to over predict radiation from localized heat sources. In fact, the DO model also tends to over predict radiation but less than the P1 model. Moreover, calculation time is the same for the P1 model and the DO model (for this problem, i.e., with the configuration that was used).

To improve the starting calculations, the radiation solver was disabled at the beginning (approximately up to the 50th iteration).

### 5.1.3 Turbulence’s model

Different variants of the K-ε model (the only one available for this problem) were tested. It was found that the standard model is the most appropriate here. There are two major problems that can occur when using the turbulence model.

When the tunnel is simulated without any fire, a logical solution would be to make a grid with very small mesh close to the wall and coarser mesh in the middle of the tunnel. However, because of the fire, the central part of the tunnel cannot be made of coarse mesh. Thus, (and because the model tunnel is relatively large) it was not possible to use small mesh close to the wall.

This resulted in a situation where no mesh was used in the viscous sublayer. The wall functions, defined by FLUENT, are not good enough to correctly solve the boundary layer. Indeed, the values of Y+ mostly go beyond 200 whereas FLUENT ’s documentation advised 30 as the most desirable value. This shows that velocity profiles are not good close to the walls. Figure 18 shows that the results will become abnormal when refining the grid close to the wall.

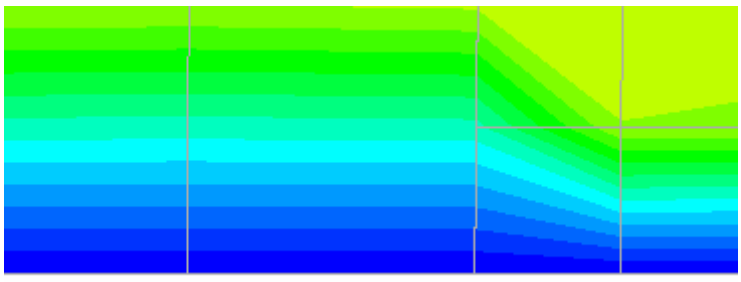

Figure 18 The calculations of the velocities will become abnormal when refining the grid close to the wall. This can be observed to the right in the figure, where the results show abnormal results.

The other problem provoked by the turbulence model used here is an inaccurate calculation of the turbulent viscosity and its effects on kerosene transport. In fact, some kerosene is not burnt at the fire location (it is however burnt further away from the fire in the solution, which makes the problem smaller).

To solve this problem the RNG was used as a standard. That allows using the option “modelling the effective viscosity, otherwise turbulent viscosity would have been over predicted. As a result, the kerosene was not blown away, and the calculation of the fire chemistry became totally wrong.

This problem was never completely solved in this study. But it was noted that if a velocity-inlet (instead of a massflow-inlet) was used as a boundary condition for the fuel-inlet, the amount of kerosene that was not consumed was reduced. Moreover, an increase of the initial temperature of the kerosene injected into the tunnel improved the solution of this problem. In Table 5 the amount of Kerosene that was not consumed at 1 m from the fuel inlet depending on the measures taken, is shown.

Table 5 The amount of Kerosene that was not consumed at 1 m from the fuel inlet depending on the measures taken.

| Solutions | Nothing done | Increasing initial temperature | Using velocity-inlet conditions |
|---|---|---|---|
| Kerosene not consumed at 1 m far from the fire (kerosene injected was 1,51 g/s) | 0.55 g/s | ➔ 0.44 g/s | ➔ 0.26 g/s |

Another way to solve this problem would have been to use refinement of the grid wherever the gradients of the mass fraction of kerosene are too high. This procedure would have prevented any comparison between different simulations since they would not have been made with the same grid.

### 5.1.4 Influence of geometry

The geometry for the fuel-inlet, has been studied with the aim to reduce the mass of kerosene which is blown away. This was never completely solved, but this study led us to understand the strong influence of the geometries on the fire behaviour (at least in modelling).

There are restrictions in modelling of the fuel-inlet because of the building of the grid with hexahedral meshes. Therefore, numerous geometries of the fuel-inlet were tested. In Table 6, a list of the geometries simulated, is given.

In Figure 19, the fuel-inlet that was chosen for the simulations is shown. This heightened case (see Table 6) is the best compromise between the quality of the result and how fast the convergence of the calculations was obtained.

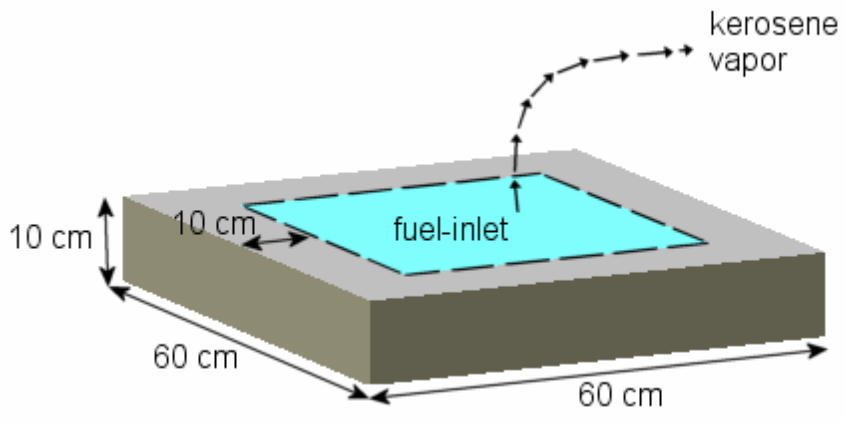


Figure 19 The best geometry in modelling the fuel-inlet.

Table 6 Different geometries of the fuel-inlet that were simulated in order to obtain a realistic combustion conditions.

**Realistic case**

Among all the geometries that were tested, this is the most realistic compared to the actual test setup. However, it is very difficult (almost impossible) to get a converged solution. Too many vortices are created close to the inlet and it seems that this phenomenon destabilises the combustion calculation.

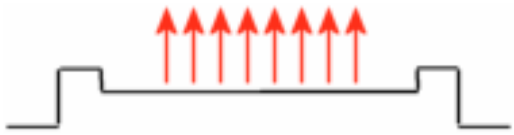

**Flat case**

This is the most simplified case. The results are promising, except for the temperature within 3 m and 6 m, downstream the fire. Comparisons were made with the case presented below.

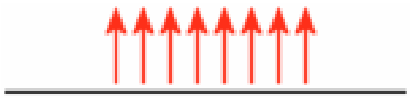

**Elevated case**

This was a good compromise. There are two possible solutions here. One is that the fuel-inlet surface is simulated as the entire area of the top surface. The other is that the fuel-inlet is only a part of the top surface. It was not easy to get a solution converged with the first variant. The second variant was analysed further, see Figure 19.

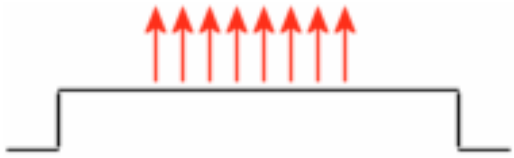

**Reducing the wind case**

The objective of these geometries was to reduce the wind which is applied directly to the fuel inlet. This will allow better combustion of the kerosene. Actually it seems that the decrease of the mass of kerosene which is blown away is not so dependent on the geometry. The disadvantage is that these cases are very different from the experimental case.

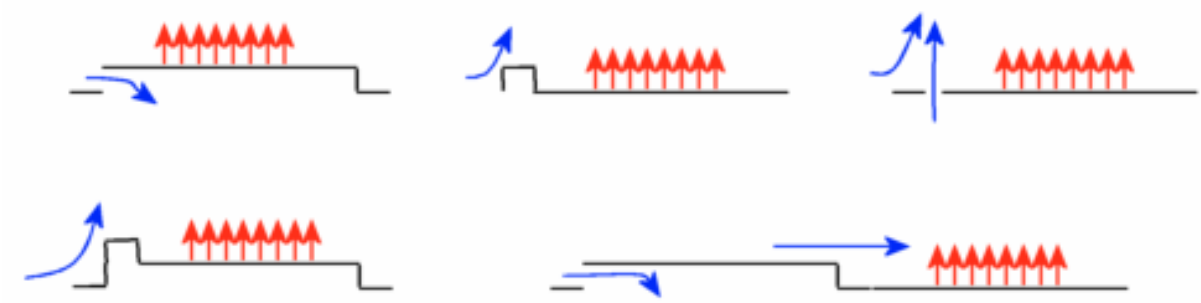

The consequences of different choices of the geometry of the fuel-inlet can be observed in Figure 20, which shows the gas temperature along the ceiling for the flat case and the elevated case, respectively. The flat case tends to underestimate temperatures along the centreline of the ceiling.

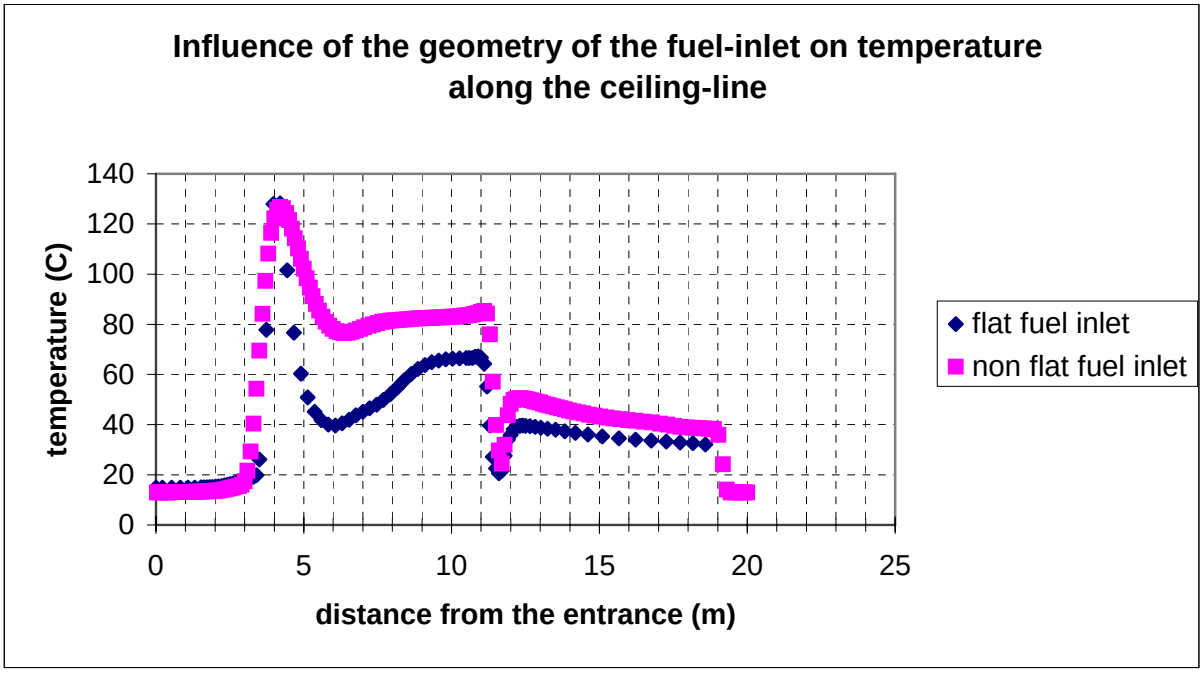


Figure 20 Strong influence of the geometry of the fuel-inlet's geometry.

The influence of the geometry on the temperature is very complicated. The main reason of this complexity is that the flow downstream the fire has to be considered in 3D. The fire plume was more spread out to the sides in the elevated case than in the flat case. The maximum temperatures are the same in both cases, but the area of the radiant surface was larger in the elevated case (see Figure 21).

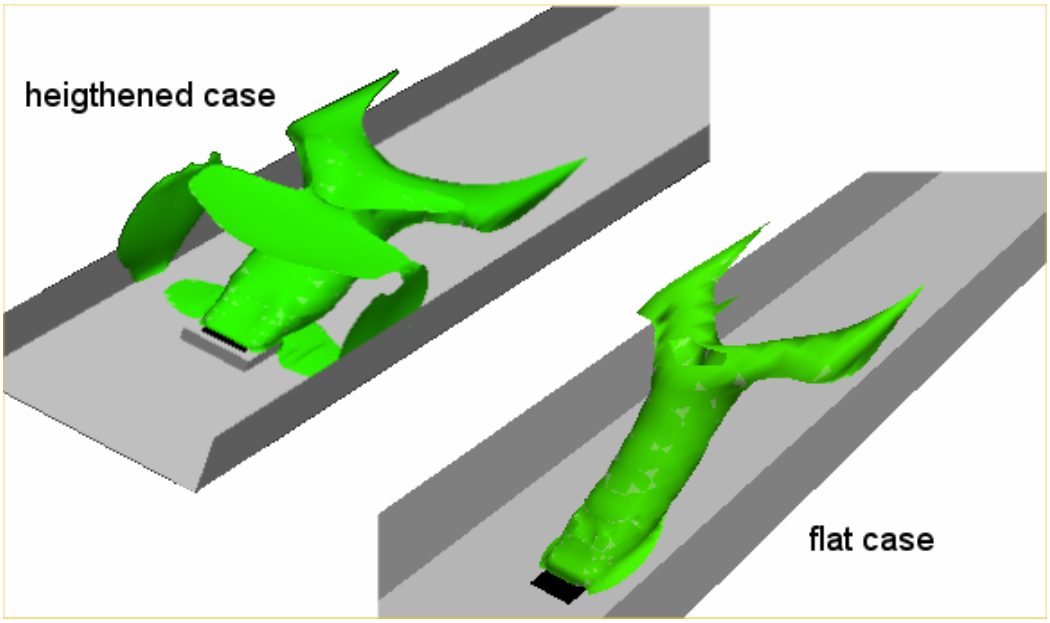


Figure 21 Iso-surfaces of temperature (100°C) at the fire location.

### 5.1.5 Consequences of strong radiation

Radiation effects are stronger in the elevated case than in other cases. Walls become hotter when absorbing radiation and consequently warm the surrounding air. Figure 22 shows the temperature, along a line 1 cm below the roof, which indicates the effects of the radiation.

Since the peak of the simulated curve and the experimental peak are exactly at the same location (on the abscissa), local experimental readings of temperature by thermocouples may have been influenced by the radiation. The gas temperatures obtained with FLUENT, along the ceiling-line 10 cm below the roof, were calculated without any adjustment for the absorption of radiation by thermocouples (indeed thermocouples not modelled). This would mean the thermocouple temperatures should be slightly higher than the calculated temperatures.

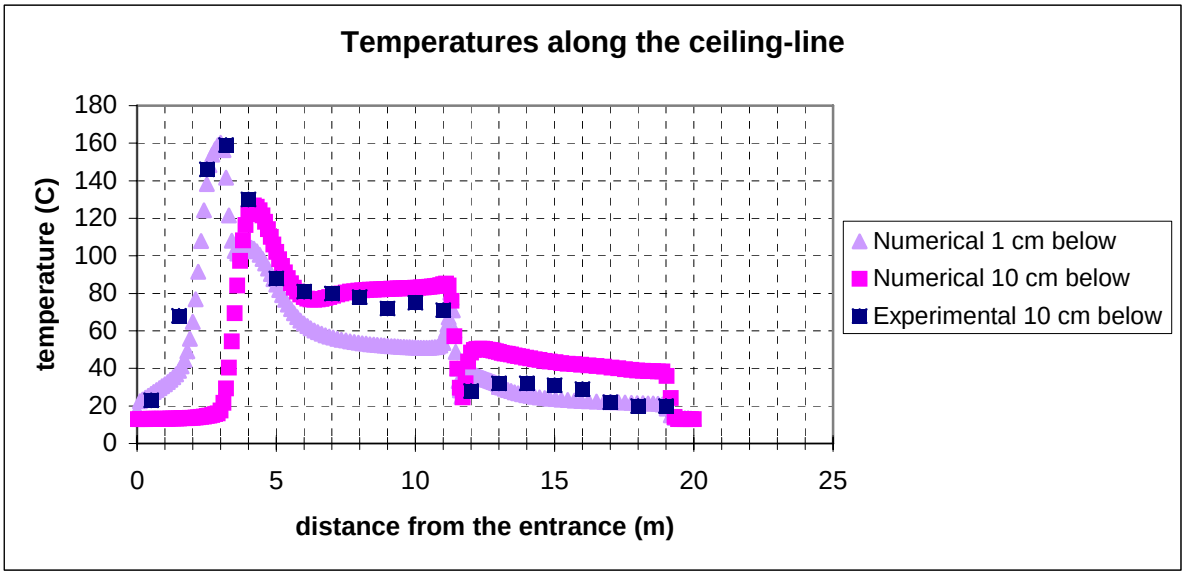


Figure 22 Radiation and convection effects can be distinguished.

## 5.2 Sensitivity of the solution

### 5.2.1 High sensitivity example

As has been pointed out earlier in the report the solution is very sensitive to the geometry of the fuel-inlet. There are also some input parameters that are important for the sensitivity of the solution. A good indicator to demonstrate this is the backlayering distance downstream the shaft. In Figure 23, an example of results which show the backlayering of is smoke layer downstream the shaft opening, is given.

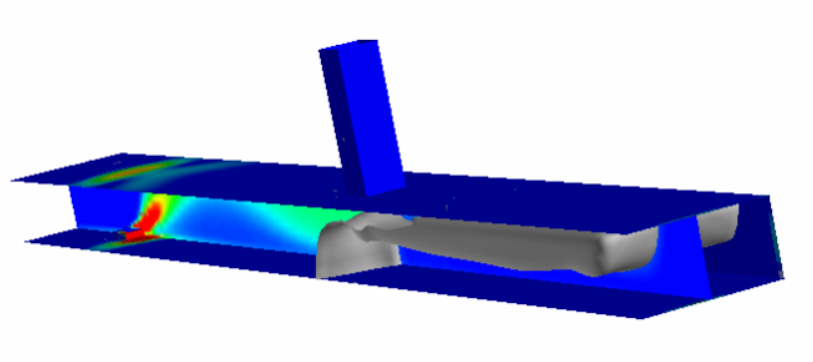

Figure 23 The backlayering downstream the shaft can be observed as a grey cloud.

If the extraction rate is increased by 10 % compared to the reference case, i.e. increase extraction rate from 3 kg/s to 3,3 kg/s, the length of the backlayering is shortened by 60 % (from 7,5 m to 3 m). If the fire is elevated by 10 cm, the temperature of the backlayering increases from 35°C to 45°C.

### 5.2.2 Local and global results

For future analysis, it is necessary to understand whether these sensitivities are related to this particular solution. The objective is to distinguish local phenomena from global phenomena (numerical or experimental). For example, the temperature of the fire could be affected by different particular flow vortices (local), whereas the energy produced by the fire is only set by the mass of the kerosene burnt (global).

According to the Figure 20 (temperature), it appears that the fire is less powerful with a flat fuel-inlet than with an elevated one. But this is not true. Actually, in the flat case, the energy is first released by the sides of the tunnel as can be seen in Figure 24 (the red colour). This means that the temperatures along the centreline of the tunnel are not representative of the heat release rate of the fire whereas in the experiments the mixture of hot and cold gases has been greater. This is essentially a local phenomena (or a three dimensional phenomena) which is very sensitive to small changes in the geometry of the model (e.g. fuel-inlet).

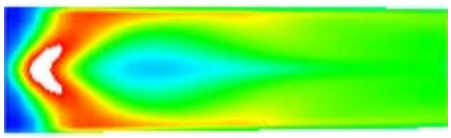

Figure 24 Flat fuel-inlet, contours of temperatures, the energy is first released by the sides of the tunnel.

The temperature of the backlayering layer is also related to a local situation. Indeed, on the left hand side of Figure 25 (flat fuel-inlet case), temperatures are mixed downstream of the fire whereas on the right hand side (elevated fuel-inlet case), temperatures are not mixed and warmer air will pass by the sides of the exhaust opening and so backlayering will be warmer.

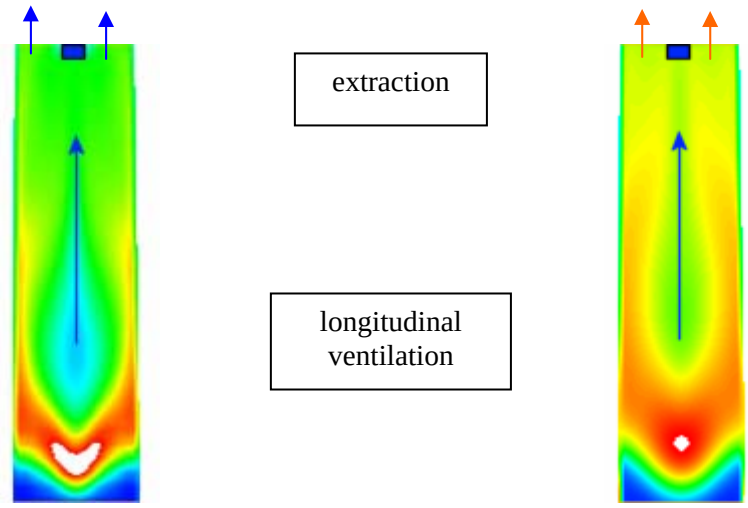


Figure 25 Temperature contours on a horizontal surface located upstream from the extraction.

It is not easy to distinguish a local result from a global result. Even if we have performed numerous numerical calculations, mostly they do not provide sufficient information to establish whether specific effects are due to local or global phenomena. However, we guess that an significant part of the results are largely due to local effects. The reason for this assumption is that the flow is very complex and several factors can be amplified by small changes.

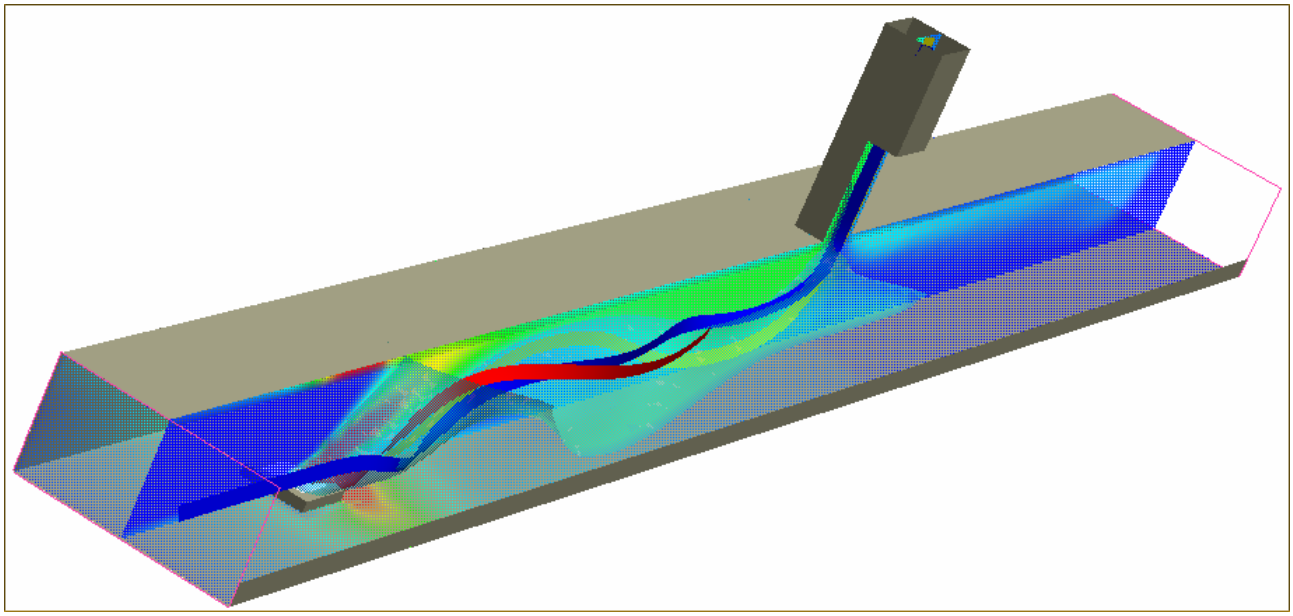

Figure 26 Example of complexity, inversion of stream-lines.

# 6 Conclusions

The aim of the study here is to investigate the possibilities and limitations of using the CFD code FLUENT for simulation of single point extraction and longitudinal ventilation. By using a simple and well defined experimental case it has been possible to understand the main phenomena, which determine the efficiency and/or the weakness of the combined system. It has been of special interest to investigate the risks and thresholds for continuous smoke spread along the tunnel when using a combined system of extraction and longitudinal flow.

CFD codes need to be “calibrated” for the type of application that they will be used for. The physical submodels available in these codes are very flexible and the choice of different parameters dependents on the type of application. A sensitivity analysis was, therefore, carried out in order to find the best combination of physical models and grid structure for the type of application used here.

From a qualitative point of view the numerical results obtained by FLUENT yield reasonable results compared to experimental ones. Local phenomenon observed during the performance of the experimental tests have been revealed by numerical simulations. Quantitatively the numerical and experimental values are somewhat different. However, these differences can be explained. First, during the experiment, temperature readings from thermocouples are altered by radiations effects. Moreover, it has been shown that the solution is very sensitive to geometrical effects.

FLUENT is apparently able to deal with the kind of problem analysed here. The numerical model used here has been presented as “the best model created” in this report. It can be applied to the next step in the study. It is, however, necessary to be aware of its limits and biases.

# 7 References

1. Ingason, H., and Werling, P., "Experimental Study of Smoke Evacuation in a Model Tunnel", FOA Defence Research Establishment, FOA-R--99-01267-311--SE, Tumba, Sweden, 1999.
2. Ingason, H., and Seco, F., "Parametric study of the efficiency of extraction system combined with a longitudinal ventilation - A numerical study using a model tunnel", Swedish National Testing and Research Institute, 2006.
3. "Memorial Tunnel Fire Ventilation Test Program - Test Report", Massachusetts Highway Department and Federal Highway Administration, 1995.
4. "FLUENT 5 User's Guide", Fluent Incorporated, 1998.

**SP Swedish National Testing and Research Institute** develops and transfers technology for improving competitiveness and quality in industry, and for safety, conservation of resources and good environment in society as a whole. With Swedens widest and most sophisticated range of equipment and expertise for technical investigation, measurement, testing and certfication, we perform research and development in close liaison with universities, institutes of technology and international partners.

SP is a EU-notified body and accredited test laboratory. Our headquarters are in Borås, in the west part of Sweden.

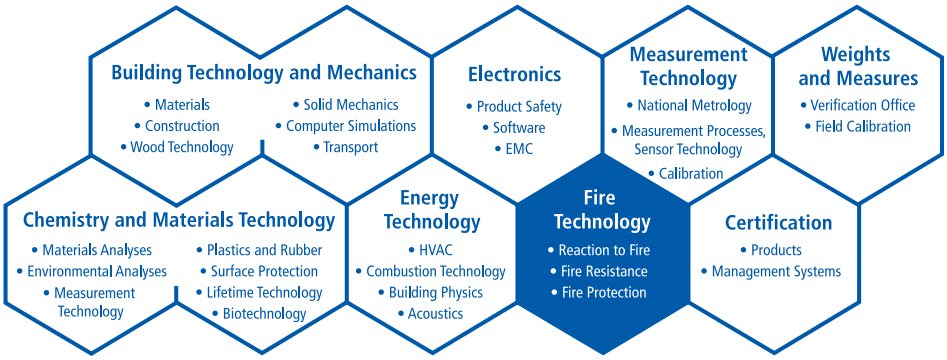


SP Fire Technology
SP REPORT 2005:47
ISBN 91-85303-79-8
ISSN 0284-5172

**SP Swedish National Testing and Research Institute**
Box 857
SE-501 15 BORÅS, SWEDEN
Telephone: + 46 33 16 50 00, Telefax: +46 33 13 55 02
E-mail: info@sp.se, Internet: www.sp.se